JOTCS A
Journal of the Turkish Chemical Society
Section: A
Chemistry
TURKISH CHEMICAL SOCIETY

Evaluation of Acetyl- and Butyrylcholinesterase Enzyme Inhibitory Activities and Cytotoxic Activities of Anthraquinone Derivatives

Funda Ozkok[1], Mehmet Boga[2], Muhammed Tuneg[2], Vildan Enisoglu Atalay[3,4], Nihal Onul[1]*, Kamala Asgarova[1], Rabia Tigli[4], Sıla Arslan[4], Dilan Akagunduz[4], Rumeysa Cebecioglu[4], Tunc Çatal[3,4]

[1]Organic Chemistry Division, Department of Chemistry, Faculty of Engineering, Istanbul University-Cerrahpaşa, Avcılar, 34320, Istanbul, Turkey.
[2]Dicle University, Faculty of Pharmacy, Department of Analytical Chemistry, 21280, Diyarbakir, Turkey.
[3]Uskudar University, Faculty of Engineering and Natural Sciences, Department of Molecular Biology and Genetics, 34662, Uskudar, Istanbul, Turkey.
[4]Istanbul Protein Research-Application and Inovation Center (PROMER), Uskudar University 34662 Uskudar, Istanbul, Turkey.

Abstract: In this study, the enzyme activity of anthraquinone compounds which were synthesized beforehand by our research group was investigated. Molecular docking studies were performed for compounds 1-(4-aminophenylthio)anthracene-9,10-dione **(3)** and 1-(4-chlorophenylthio)anthracene-9,10-dione **(5).** Compound **3** was synthesized from the reaction of 1-chloroanthraquinone **(1)** and 4-aminothiophenol **(2).** Compound **5** was synthesized (1) from the reaction of 1-chloroanthraquinone **(1)** and 4-chlorothiophenol **(4).** Anthraquinone analogs **(3, 5)** were synthesized with a new reaction method made by our research group (2). Inhibitory effects of compounds **3** and **5** were investigated against acetylcholinesterase (AChE) and butyrylcholinesterase (BuChE) enzymes which are related to Alzheimer's Disease (AD). Compounds **3** and **5** exhibited strong anti-acetyl- and butyryl-cholinesterase inhibition activities than galanthamine used as standard compound (92.11±1.08 and 80.95±1.77 %, respectively). The E_{HOMO}-E_{LUMO} values, molecular descriptors, and the calculated UV-Vis spectra of anthraquinone derivatives were computed by B3LYP/6-31+G(d,p) levels in the $CHCl_3$ phase. Based on the fluorescence property of the anthraquinone skeleton, the fluorescence activity of the bioactive anthraquinone analogue (**5**) was investigated. MTT test was performed to determine the cytotoxic effects of thioanthraquinone molecules **3** and **5**. In MTT analyses, 3 compounds showed the highest effect against Ishikawa cells at a dose of 10 µg/mL, while compound **5** showed the highest effect at a dose of 50 µg/mL. The cell viability for compound **3** was 84.18% for 10 µg/mL and the cell viability for compound **5** was 75.02% for 50 µg/mL.

Keywords: Anthraquinone, cytotoxicity, anti-Alzheimer, in-silico, thioanthraquinone.

Submitted: July 06, 2021. **Accepted:** May 10, 2022.

Cite this: Ozkok F, Boga M, Tuneg M, Enisoglu Atalay V, Onul N, Asgarova K, et al. Evaluation of Acetyl- and Butyrylcholinesterase Enzyme Inhibitory Activities and Cytotoxic Activities of Anthraquinone Derivatives. JOTCSA. 2022;9(3):729–40.

DOI: https://doi.org/10.18596/jotcsa.963290.

***Corresponding author. E-mail:** yilm@istanbul.edu.tr , Tel: (+90 212 473 70 70)

INTRODUCTION

Anthraquinones are cyclic compounds that have a class of conjugated cyclic diketones and play an active role due to electrochemical activity of main skeleton in biological and organic reactions. Anthraquinones and their analogs have applications in many areas such as medicine, pharmacy, chemistry, and material engineering (3-10). Anthraquinones can have estrogenic activity. In a study (11) with hydroxyl anthraquinones, Emodin compound having hydroxyl groups showed estrogenic activity. The discovery of important anti-cancer drugs such as Daunomycin, Adriamycin, and Mitoxantrone has led scientists to investigate anthraquinone and its derivatives that have an anti-cancer effect, especially biological activity (12-15). Damnacanthal, which is a natural bioactive compound isolated from phenolic phase of noni roots, may be found in Rubiaceae plants, too (16-17). Damnacanthal is defined as the most powerful selector inhibitor of p56Ick tyrosine kinase which is a protein activity that plays key role in chemotactic reaction of T cells to CXCL12 (18-19). Additionally, an active anthraquinone analogue, Damnacanthal, may also inhibit other tyrosine kinases (PDGFR, erbB2, EGFR and insulin receptor) in their IC50 values in micromolar concentration aperture (18). It was established in studies that Damnacanthal is also a powerful inhibitor of c-Met and acts as an antitumoral agent against hepatocellular carcinoma (20). Anthraquinone compounds, especially daunoribicin, doxorubicin, epirubicin and mitoxantrone, are the most effective clinical anticancer medications (21). Mitoxantrone, with its planar anthraquinone structure, is a clinically useful antineoplastic agent (22-28) SZ-685C, one of sea anthraquinone metabolites, represses human breast cancer and human nasopharyngeal carcinoma cells (29). Anthraquinones have high antitumor effect. They are responsible for conjunction of DNA double-helix to DNA, interactions via interpolation and decomposition, direct membrane effects, DNA damage, topoisomerase II inhibition, production of free radicals such as reactive oxygen species (ROS), apoptosis induction through topoisomerase inhibition and production of functional p53 and ROS. Additionally, anthraquinones trigger (c-Jun N terminal kinase) Akt / PKB (Protein Kinase B) through JNK and apoptosis through mitochondrial paths (29-35). Cholinesterase enzymes (acetyl and butyryl) in the central nervous system are responsible for the termination of cholinergic signaling by hydrolyzing the neurotransmitter acetylcholine (ACh). In the brain, decreased levels of ACh with the loss of cholinergic neurons leads to memory loss and progressive cognitive decline, which are common symptoms of Alzheimer's disease (AD) (36). Although the reason of AD is unknown, many studies have reported that ACh levels have been exhausted in patients suffering from AD. AChE and BuChE inhibition is an effective mechanism for the treatment of AD (37-38). According to the results of our literature review, there are several cholinesterase inhibitors namely galanthamine, rivastigmine, donepezil, and tacrine used for the treatment of AD. Therefore, the above mentioned drugs possess constricted efficacy, toxicity, and have unfavorable side effects such as diarrhea, vomiting, dizziness, hepatotoxicity, and nausea (39), so there is a need for more potent and highly efficient cholinesterase inhibitors for the treatment of AD. According to literature surveying, there are a few studies about anticholinesterase activity studies on anthraquinone compounds (40-43) but there is not any study about thioanthraquinone compounds except for the study of Tonelli et al. (44), in which only one thioanthraquinone compound was investigated for anticholinesterase activity. This study is important to examine the properties of anti-acetyl and butyrylcholinesterase inhibitory activities for thioanthraquinone compounds. In this study, synthesis was done via a method (2) that had been discovered by our team prior to this study, enzyme activities of anthraquinone analogs were examined and molecular docking studies of analogs were performed. Moreover, cytotoxicity studies of thioanthraquinone molecules were also conducted in the study.

MATERIALS AND METHODS

Chemistry

General

All chemicals were purchased from either Sigma-Aldrich or Merck. Solvents, unless otherwise specified, were of reagent grade and distilled once prior to use. Thin layer chromatography was performed on Merck (60 F 254) TLC-plates (aluminum-based). Melting points were measured on a Buchi B-540 apparatus and were uncorrected. Mass spectra were recorded on Shimadzu LCMS-8030 triple quadrupole spectrometer in ESI (+) polarity.

Synthesis

In this study, compounds **3** and **5** were synthesized in a previous study (1). Various bioactive amino- and thioanthraquinone analogues were synthesized in our previous studies (45-46). In this work, enzyme, *in silico* and *in vitro* study of these compounds were performed. Our target molecule 1-(4-chlorothiophenyl)-anthracene-9,10-dione (**3**) was obtained from reaction of starting material 1-aminoanthraquinone (**1**) and 1-(4-aminothio)phenol (**2**) according to a patent method (2). A yellowish reaction mixture was obtained at the end. 10 mL of aquous potassium hydroxide solution was added to this mixture, and the reaction temperature was raised to 120–130

°C. After reflux (48 h), an orange crystal thio-anthraquinone compound (**3**) was obtained. The new product (**3**) was extracted with chloroform (30 mL). The organic layer was washed with water and dried with calcium sulfate. The synthesized novel analogue (**3**) was purified by column chromatography. Another target molecule 1-(4-chlorophenylthio)anthracene-9,10-dione (**5**) was obtained from reaction of starting material 1-aminoanthraquinone (**1**) and 1-(4-chlorothio)phenol (**4**) according to a patent method (2). A yellowish reaction mixture was obtained at the end. 10 mL of aquous potassium hydroxide solution was added to this mixture, and the reaction temperature was raised to 120–130 °C. After reflux (48 h), an orange crystal thio-anthraquinone compound (**3**) was obtained. The new product (**5**) was extracted with chloroform (30 mL). The organic layer was washed with water and dried with calcium sulfate. The synthesized novel analogues (**3**, **5**) were purified by column chromatography. The chemical structure of novel thio-anthraquinone compounds (**3, 5**) were characterized by spectroscopic methods such as FT-IR, NMR, MS, and (UV)–visible spectrophotometry. Synthesized analogs **3** and **5** were shown in Figure 1.

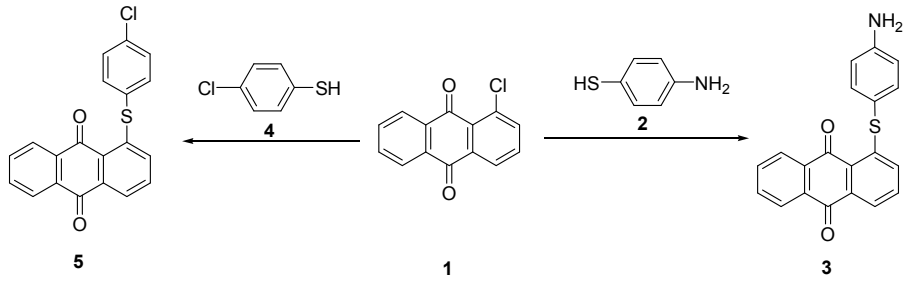

Figure 1: Illustrations of thioanthraquinone analogs in this study.

(**3**): Orange crystal, mp: 227-228 °C. Yield: 0.76 g (52%). Rf [Petroleum ether/chloroform (1:1)]: 0.43. IR (KBr, cm^{-1}): υ= 3021, 2913 (C-Harom), 1594 (C=C), 1647 (C=O). UV-vis($CHCl_3$): λmax (logε)= 3.79 (427 nm), 4 (302 nm), 4.63 (247 nm). ^1H NMR (499.74 MHz, $CDCl_3$): δ= 7.29-8.17 (m, 4H, Harom). ^{13}C NMR (125.66 MHz, $CDCl_3$): δ= 123.27, 125.95, 126.47, 127.21, 129.33, 129.53, 130.69, 131.64, 131.92, 132.87, 133.38, 134.14, 135.30, 136.10, 136.34, 144.69 (C_{arom} and CH_{arom}), 181.93 (C=O). $C_{20}H_{11}O_2SCl$, (M, 350.82 g/mol).

(**5**): Red solid, mp: 208-209 °C. Yield: 0.78 g (57%). Rf [Petroleum ether/chloroform (1:1)]: 0.48. IR (KBr, cm^{-1}): υ= 2923, 2852 (C-Harom), (C=C), (C=O). UV-Vis ($CHCl_3$): λmax (logε)= 3.77 (430 nm), 4.04 (303 nm), 4.71 (249 nm). ^1H NMR (499.74 MHz, $CDCl_3$): δ= 6.69-6.71 (m, 4H, Harom), 7.09-8.30 (m, 7H, Harom). ^{13}C NMR (125.66 MHz, $CDCl_3$): δ= 125.83, 126.46, 127.79, 130.76, 131.62, 131.67, 132.64, 133.07, 133.27, 134.09, 136.11, 136.59, 147.10, 147.32 (C_{arom} and CH_{arom}), 182.23 (C=O). $C_{20}H_{13}NO_2S$, (M, 331.39 g/mol).

Fluorescence Analysis

In this study, fluorescent spectra for **5** have been investigated. Anthraquinone skeleton as a rigid structure is very effective in fluorescent behavior of compound **5**. There is a π-bond delocalization in aromatic thiosubstituted anthraquinone structure. Additionally, carbonyl groups in the structure of molecules are strong withdrawing groups. Aromatic thiosubstituted group in compound **5** amplifies fluorescence aspect of anthraquinone. In the fluorescence spectrum of **5**, excitation and emission wavelengths were observed at 435 nm ($\lambda_{exc.}$) and 683 nm ($\lambda_{em.}$), respectively. Fluorescence spectrum of thiosubstituted anthraquinone compound **5** is shown in Figure 2.

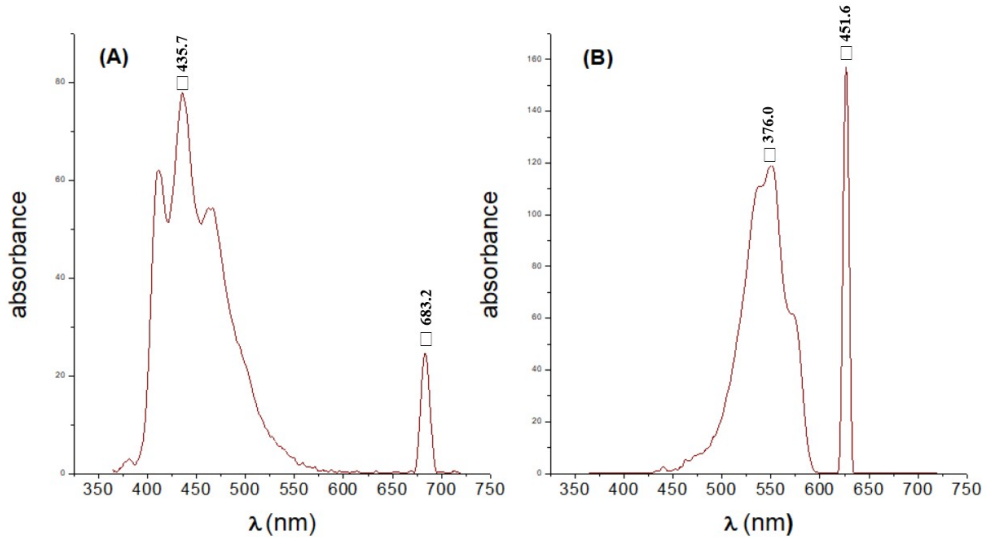

Figure 2: Excitation (left) and emission spectrum (right) of **5** ($2.0x10^{-3}$ M) in $CHCl_3$ solution.

Anticholinesterase activity

The acetyl-cholinesterase and butyryl-cholinesterase inhibitory activities of the compounds **3** and **5** were tested by using a slightly modified Ellman method (47). Acetylthiocholine iodide (or butyrylthiocholine iodide) was used as substrate of the reaction and DTNB (5,5'dithiobis nitrobenzoic acid) was used for the measurement of the anticholinesterase activity. Galanthamine was used as the standard drug. 130 µL of sodium phosphate buffer (pH 8.0), 10 µL of 4 mM sample solution and 20 µL of AChE (or BChE) solution were mixed in each well and incubated for 15 min at 25 °C. The reaction was then initiated by the addition of 10 µL of DTNB and 10 µL of acetylthiocholine iodide (or butyrylthiocholine iodide). Final concentration of the tested solutions was 200 µg/mL. The hydrolysis of these substrates was monitored using microplate ELISA reader XS by the formation of yellow 5-thio-2-nitrobenzoate anion as the result of the reaction of DTNB with thiocholine, released by the enzymatic hydrolysis of acetylthiocholine iodide or butyrylthiocholine iodide, at a wavelength of 412 nm.

$$\%\text{Inhibition} = (A_{Cont} - A_{Sample})/A_{Cont} \times 100,$$

where A_{Cont} is the absorbance of the control and A_{Sample} is the absorbance in the presence of the sample

Cell Culture

*Preparation of the extracts of compounds **3** and **5***

To prepare 10 mg/mL concentration of compound **3** and **5**, 10 mg of the compounds were weighed and transferred into a sterile Eppendorf and 1 mL of 100% methanol (CH_3OH) was added into the tube. This mixture was dissolved by an ultrasonicator at 65 °C for 15 minutes and vortexed for 2 minutes and this process was repeated 3 times. The stock solutions of compounds **3** and **5** were prepared in this way. After the stock solutions, doses were prepared for MTT Assay by serial dilution methods such as 500 µg /mL, 100 µg /mL, 50 µg /mL, 10 µg /mL, 5 µg /mL and 1 µg /mL with serum-free medium.

Human endometrial adenocarcinoma cell line (Ishikawa) and human endothelial cell line (ECV304) were used in the study. The cells were cultured in DMEM medium (Gibco, 11960044, UK) supplemented with 10% of fetal bovine serum (Gibco), 1% penicillin/streptomycin, and L-glutamate at 37 °C in a humidified atmosphere of 5% CO_2. Ishikawa cells and ECV 304 were grown in 35-mm culture dishes for 24 h before the experiments. Cells were diluted to 10^5 cells /mL with Gibco DMEM (1x) medium.

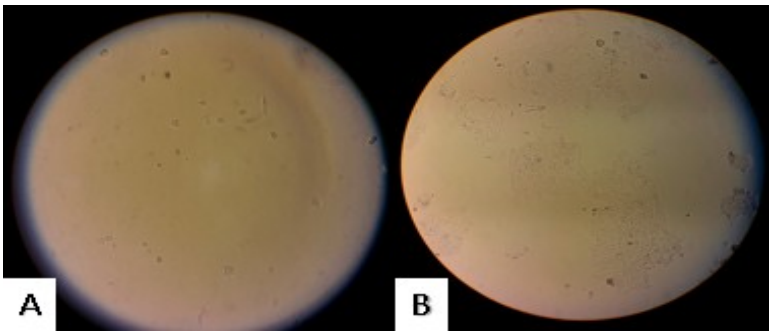

Figure 3 (A): Microscopic view of Ishikawa (x10*)*. **Figure 3 (B):** Microscopic view of ECV 304 (x10).

Cytotoxicity Assay

To determine the cytotoxic effect of **3** and **5** extracts on the cells' MTT assay ((3- (4,5-dimethyl thiazole-2-yl)-2,5-diphenyl tetrazolium bromide), 90 µL of cell- medium with serum mixture was added to have 9000 cells in each well within Nest 96 Well Plate. The 96 Well Plate is incubated at 37 °C and 5% CO_2 for 24 hours. After this period, 10 µL of **3** and **5** solutions in different concentrations that were suitable for each well were added. The 96 Well Plate is incubated at 37 °C and 5% CO_2 for 24 hours. After 24 hours, 10 µL of MTT (Invitrogen, Cat No: M6494). Solution with stock concentration 5 mg/mL and prepared in sterile PBS was added to each well. The 96 Well Plate is incubated at 37 °C and 5% CO_2 for 3 hours, after which 90 µL was discarded from the wells without touching the cells and 100 µL 50% DMSO (VWR, Cat No: 23500.322)- 50% Isopropanol (VWR, Cat No: 20842.323) was added on each well. The surface of the 96 Well Plate was covered with aluminum foil. The 96 Well Plate was left at room temperature for 45 minutes. Then, 96 Well Plate was measured at 570 nm with a spectrophotometer. Cytotoxicity index (CI) was calculated to following formula;

CI %(Cytotoxicity index) = 1- OD treated wells / OD control wells X 100

Computational Methods

The conformer analysis of synthesized compounds were performed to find the stable structures with a semi-empirical PM6 method (48-49) using the program Spartan'16 v1.1.4 (Spartan'16 Wavefunction, Inc. Irvine, CA.). The calculated most stable structures were optimized with a semi-empirical PM6 method, for the better geometries optimized structures made *re*-optimize and were obtained UV-Vis Spectra with the Density Functional Theory (DFT) B3LYP (Becke's Three Parameter Hybrid Functional using the Lee, Yang and Parr Correlation Functional) (50) with the 6-31+G(d,p) method in the gas and $CHCl_3$ phases with the IEF-PCM approach (51).

The E_{HOMO}-E_{LUMO} were calculated using time-dependent density functional theory (TD-DFT) at the B3LYP/6-31+G(d,p) levels in $CHCl_3$ phase, which was done by using the Self-Consistent Reaction Field (SCRF) method. At the same time molecular descriptors such as electronegativity (χ), electron affinity (*A*), hardness (*η*), softness (*S*), electrophilicity index (ω) must be defined by the same computational methods. There is a practical calculation method to calculate for chemical hardness (*η*) and electronegativity (χ) (Eq. 1), as given by Parr and Pearson (52-53).

$$\eta \approx (I-A)/2 \qquad x \approx (I+A)/2 \qquad \text{(Eq. 1)}$$

where I is the ionization potential and A is the electron affinity. The Koopman's theorem was used for the calculation of I and A values derived from the frontier orbital energies of optimized neutral molecules, according to this theorem $I = -E_{HOMO}$ and $A = -E_{LUMO}$. Using Koopman's theorem, the chemical hardness and electronegativity are defined in terms of orbital energies (Eq. 2):

$$\eta \approx (E_{LUMO} - E_{HOMO}) / 2$$
$$x = -\mu \approx -(E_{LUMO} - E_{HOMO}) / 2 \qquad \text{(Eq. 2)}$$

The ω and *S* values are calculated by the following Eq. 3:

$$\omega \approx \mu^2/2\eta, \qquad S \approx 1/(2\eta) \qquad \text{(Eq. 3)}$$

All visualizations and calculations were carried out with the methods implemented in GaussView5.0 (54) and Gaussian 09 package (55)

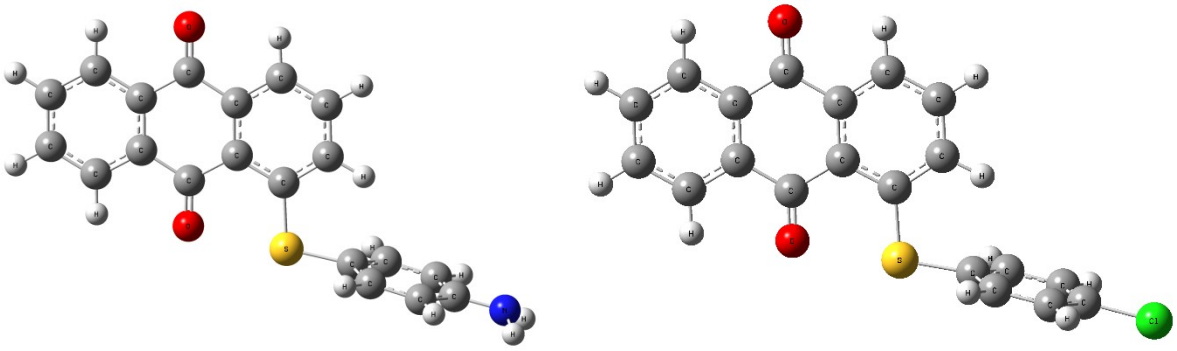

Figure 4: Optimized structures of the synthesized anthraquinone derivatives: **3** (left), **5** (right).

RESULTS

Chemistry

Characterization of synthesized compounds

1-(4-Aminothiophenyl)-anthracene-9,10-dione (3): M.p: 187-188 °C

1-(4-Chlorothiophenyl)-anthracene-9,10-dione (5): M.p: 192-193 °C

Biochemical results

Enzyme Activity

The acetylcholinesterase (AChE) and butyrylcholinesterase (BChE) enzyme inhibitory activities were evaluated for the determination of the therapeutic potential of the compounds **3** and **5** for the treatment of Alzheimer's disease (AD). The inhibition of AChE and BChE were given as percentage at 200 µg/mL concentration in Table 1 and compared with the galanthamine which is used as a standard drug. Compounds **3** and **5** demonstrated strong anti-acetyl and anti-butyrylcholinesterase activities better than galanthamine. While the galanthamine showed 80.03±1.04 and 84.54±0.39%, acetyl and butyrylcholinesterase inhibition, respectively, compound **5** exhibited 80.95±1.77 and 93.67±1.01% inhibition. Compound **3** is stronger than compound **5** and galanthamine with 92.11±1.04 inhibition against acetylcholinesterase enzyme. Also compound **3** showed weak butyrylcholinesterase inhibitory activity.

Table 1. Enzyme inhibition activities of samples and standard compound.

Samples	Inhibition %[a] AChE	BChE
3	92.11±1.08	35.25±0.36
5	80.95±1.77	93.67±1.01
Galantamine[b]	80.03±1.04	84.54±0.39

[a] 200 µg/mL
[b] Standard compound
NA: Not Active

In the study of Tonelli et al. (44), only one thioanthraquinone compound named 1-{[(1R,9aR)-(octahydro-2H-quinolizin-1-yl)methyl]thio}-9,10-anthraquinone, was synthesized and investigated for its anticholinesterase activities. This compound showed moderate inhibitory activity against acetyl and butyrylcholinesterase enzymes with IC_{50}:3.6 µM and 3.4 µM values, respectively. Therefore, there is no literature about anticholinesterase activity of thioanthraquinone compounds except for the study of Tonelli et al. (44) presented study is very important in this respect.

In vitro

MTT Assay was applied to the cells with methanol (CH_3OH) extract prepared from compound **3** and compound **5** with a stock concentration of 10 mg/mL. As cell lines, Vessel Endothelial Cell Line ECV304 and Human Endometrial Adenocarcinoma Cell Line Ishikawa were used.

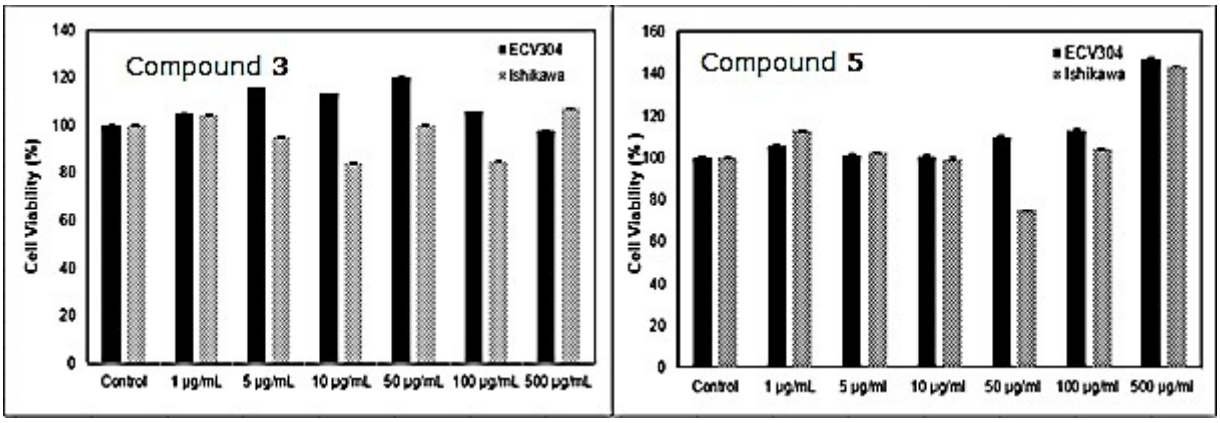

Figure 5: MTT Assay Results of **3** and **5**.

According to these results, the cell viability of **3** on ECV304, the healthy cell line of Methanol (CH_3OH) extract was calculated as 105.02% at 1 µg /mL dose and 97.69% at 500 µg /mL dose. On the cancer cell line Ishikawa, it was calculated as 104.43% at 1 µg /mL dose and 106.92% at 500 µg /mL dose. According to MTT Assay results, **3** was determined as at 10 µg/mL dose was the most effective on Ishikawa and cell viability at this dose was measured as 84.18%. Also, at 50 µg/mL dose was the most effective on ECV304 and cell viability at this dose was measured as 120.20%. The cell viability of compound **5** on ECV304, the healthy cell line of Methanol (CH_3OH) extract was calculated as 105.45% at 1 µg /mL dose and 147.14% at 500 µg /mL dose. On the cancer cell line Ishikawa, It was calculated as 112.79% at 1 µg /mL dose and 143.52% at 500 µg /mL dose. According to MTT Assay results, **3** was determined as at 10 µg/mL dose and **5** was determined as at 50 µg/mL was the most effective on Ishikawa. Cell viability at 10 µg/mL dose was measured as 84.18% and cell viability at 50 µg/mL dose was measured as 75.02%. Compound **3** was determined as at 50 µg/mL dose and compound **5** was determined as at 500 µg/mL was the most effective on ECV304. Cell viability at 50 µg/mL dose was measured as 120.20% and cell viability at 500 µg/mL dose was measured as 147.14%.

DISCUSSION

In this study, which aims to determine and analyze the synthesized compounds by quantum chemical methods. The HOMO-LUMO distribution and bandgap values for synthesized compounds were calculated by theoretical methods gathered in gas and $CHCl_3$ phases (Figure 6). The E_{HOMO}-E_{LUMO} are responsible to ionization potential and electron affinity. The energy values, E_{HOMO}-E_{LUMO} bandgap, and distribution of the HOMO-LUMO are a crucial point of stability for the molecules. The small band gap points to the compound called polarized and soft molecule. For the studied molecules, the HOMO's are mainly localized on the sulfur and surrounding atoms, whereas the LUMO's are distributed within the cyclic structures of the molecule. This means that the aromatic group in the molecule would be more easily attacked. The other important result is solvent effect, the E_{HOMO}-E_{LUMO} bandgaps for the studied **3** and **5** molecules in the $CHCl_3$ phase are 0.10512 and 0.11962 eV, respectively, are smaller than in the gas phase. The results depicts that the molecules in the solvent have a stronger electron donating ability.

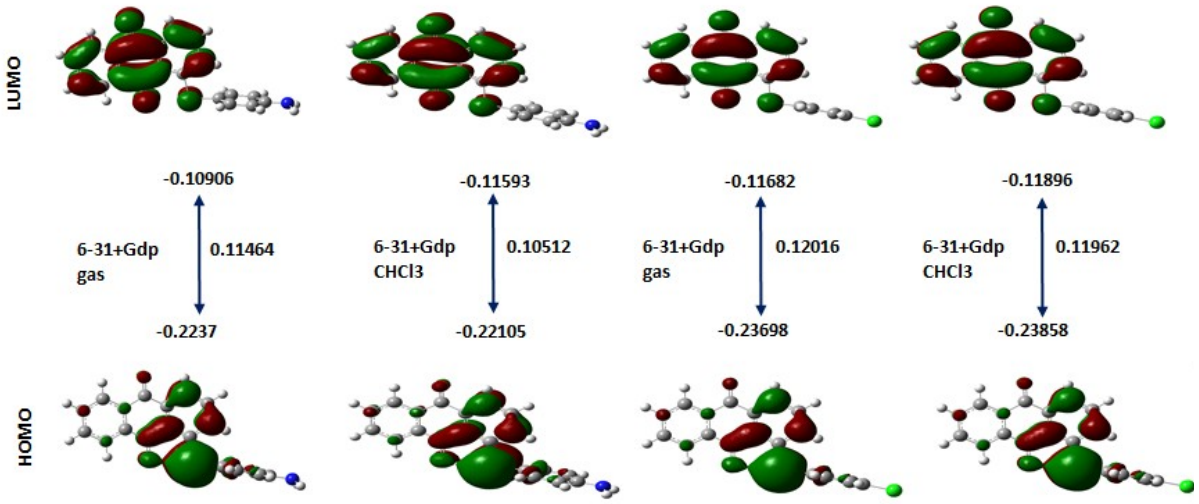

Figure 6: E_{HOMO} and E_{LUMO} levels along with bandgap values (eV) in the gas and $CHCl_3$ phases obtained by TD-DFT//B3LYP/6-31+G(d, p) method of the studied compounds.

Molecular identifier values obtained from the total energy for the **3** and **5** molecules in gas and $CHCl_3$ solvents are listed in Figure 6. The η is one-half the HOMO–LUMO gap of the molecules, the meaning is the larger gap the greater hardness and stability. This property is therefore a powerful identifier that hard molecules are less reactive than softer molecules. Table 2 shows that hardness is affected by solvent, the molecules **3** and **5** have larger hardness value in when dissolved in $CHCl_3$, as hard molecules are less reactive than softer molecules (56); the stability order is therefore $CHCl_3$>gas phase. Low chemical potentials for the molecules are causing a good electrophile, while an extremely hard molecules have feeble electron acceptability. Electrophilicity depends on both the chemical potential and hardness (57) The obtained χ and ω values show that the polar solvent contributes to accentuate the parametric representation of activity. We observed in this study and our previous studies (58-59) that solvent phase and selection have a considerable effect on electrophile/nucleophile interactions.

Table 2: Calculated Molecular identifier, E_{HOMO} and E_{LUMO} as well as band gap energy (eV) values of the studied compounds by TD-DFT//B3LYP/6-31+G (d, p) method in gas and $CHCl_3$ phases.

Compound	Solvent	Molecular Descriptors								
		E_{HOMO}	E_{LUMO}	ΔE	A	I	η	χ	ω	S
3	Gas	-0.2237	-0.1091	0.1146	0.2237	0.1091	-0.0573	0.1664	-0.2415	-8.7229
	$CHCl_3$	-0.2211	-0.1159	0.1051	0.2211	0.1159	-0.0526	0.1685	-0.2701	-9.5129
5	Gas	-0.2369	-0.1168	0.1202	0.2369	0.1168	-0.0601	0.1769	-0.2604	-8.3222
	$CHCl_3$	-0.2386	-0.1189	0.1196	0.2386	0.1189	-0.0598	0.1787	-0.2672	-8.3598

The calculated UV-Vis spectra for **3** and **5** molecules with the DFT//B3LYP/6-31+G(d,p) method in the gas and $CHCl_3$ phases are given in Figure 7 below. The Figure 7 depicted that the excitation energies are effected by solvent phase, an average energy shifts were calculated for each molecule.

Phase	Compounds	
	3	**5**
Gas	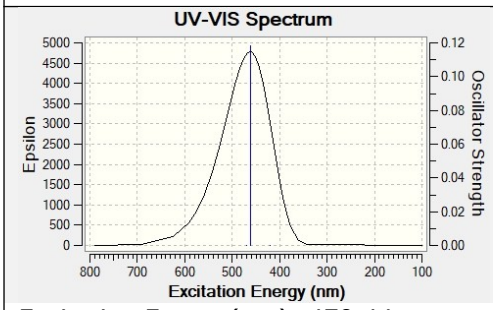 Excitation Energy(nm): 470.44 Oscillatory Strength: 0.0001	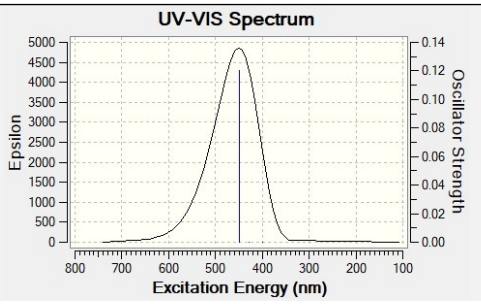 Excitation Energy(nm): 417.37 Oscillatory Strength: 0
$CHCl_3$	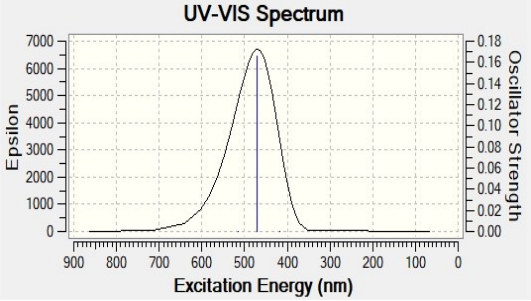 Excitation Energy(nm):514.18 Oscillatory Strength: 0	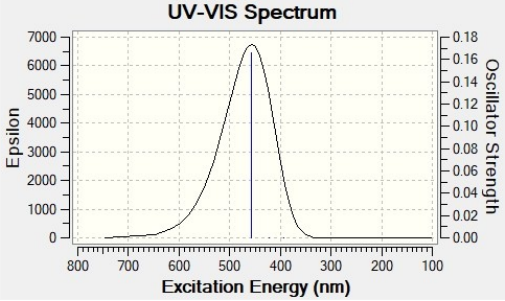 Excitation Energy(nm): 456.39 Oscillatory Strength: 0.1664

Figure 7: Calculated UV-VIS spectra for **3** and **5** molecules.

CONCLUSIONS

The investigated compounds having anthracene-9,10-dione skeletal structure showed very good anti-Alzheimer's activity, the potential of being drug candidates for anti-Alzheimer's treatment of compounds **3** and **5** and the same skeletal structures should be explored in more detail. Although compounds **3** and **5** did not show any significant results on Ishikawa, the dose of compound **3** at a concentration of 10 µg/ mL increased the cytotoxic level. Also, the dose of compound **5** at a concentration of 50 µg/ mL increased the cytotoxic level. The dose of compound **3** at a concentration of 50 µg/mL and the dose of compound **5** at a concentration of 500 µg/mL on ECV304 increased proliferation. The value of the E_{HOMO}, E_{LUMO} and band gap energies produce a crucial information about investigated compounds in the gas and $CHCl_3$ phases. **3** compound is determined more stable molecule than **5** according to the E_{HOMO}-E_{LUMO} bandgap (0.1051 eV) in the $CHCl_3$, indicating that the molecule in $CHCl_3$ solvent has stronger electron donating ability. Thioanthraquinone analogs compound **3** and **5** showed remarkable biological activity results. Thioanthraquinone derivatives formed via reaction of anthraquinones and thiols are very limited in the literature. Within this scope, when both the specificity of and the biological activity potential of thioanthraquinone compounds are taken into consideration, these may be expected to be a good medication molecule candidate.

ACKNOWLEDGMENTS

This study was funded by Scientific Research Projects Coordination Unit of Istanbul University-Cerrahpasa. Project number:45266.

CONFLICT OF INTERESTS

The authors declare that there are no conflict of interests.

REFERENCES

1. Haciosmanoglu E, Ozkok F, Onsu AK, Bektas M, Varol B, Pehlivan S. Synthesis of New Anthraquinone Derivatives and Anticancer Effects on Breast Cancer Cell Lines. Eurasia Proc Sci Technol Eng Math. 2018 Dec 4; (4):271–6.

2. Ozkok F, Sahin YM. BİYOAKTİF ANTRAKİNON ANALOGLARI VE BUNLARIN SENTEZİNE YÖNELİK METOT. 2016/19610. p. https://portal.turkpatent.gov.tr/anonim/arastirma/patent/dosya-takibi.

3. Kshirsagar AD, Panchal PV, Harle UN, Nanda RK, Shaikh HM. Anti-Inflammatory and Antiarthritic Activity of Anthraquinone Derivatives in Rodents. Int J Inflamm. 2014;2014:1–12.

4. DemiRezer LO, Uzun M, Ozenver N, Guvenalp Z. Determination of Phytoestrogenic Potential of Anthranoids by Molecular Docking Studies. :1.

5. Aulenta F, Ferri T, Nicastro D, Majone M, Papini MP. Improved electrical wiring of microbes: anthraquinone-modified electrodes for biosensing of chlorinated hydrocarbons. New Biotechnol. 2011 Dec;29(1):126–31.

6. Kang D, White RJ, Xia F, Zuo X, Vallée-Bélisle A, Plaxco KW. DNA biomolecular-electronic encoder and decoder devices constructed by multiplex biosensors. NPG Asia Mater. 2012 Jan;4(1):e1–e1.

7. Mariappan K, Basa PN. Coordination polymers of 1,8-bis(2-methylthioethoxy)anthraquinone and 1,5-bis(2-methylthioethoxy)anthraquinone with Ag(I): Synthesis and X-ray crystallography. Inorganica Chim Acta. 2011 Jan;366(1):344–9.

8. Chang M-Y, Tai H-Y. Synthesis of 2-substituted 9,10-anthraquinones. Synth Commun. 2013 Dec 17;43(24):3363–72.

9. Jarrahpour A, Ebrahimi E, Khalifeh R, Sharghi H, Sahraei M, Sinou V, et al. Synthesis of novel β-lactams bearing an anthraquinone moiety, and evaluation of their antimalarial activities. Tetrahedron. 2012 Jun;68(24):4740–4.

10. Liang D, Su Z, Tian W, Li J, Li Z, Wang C, et al. Synthesis and screening of novel anthraquinone−quinazoline multitarget hybrids as promising anticancer candidates. Future Med Chem. 2020 Jan;12(2):111–26.

11. Li F, Li X, Shao J, Chi P, Chen J, Wang Z. Estrogenic Activity of Anthraquinone Derivatives: In Vitro and In Silico Studies. Chem Res Toxicol. 2010 Aug 16;23(8):1349–55.

12. Dimarco A, Gaetani M, Orezzi P, Scarpinato BM, Silvestrini R, Soldati M, et al. "DAUNOMYCIN", A NEW ANTIBIOTIC OF THE RHODOMYCIN GROUP. Nature. 1964 Feb 15;201:706–7.

13. White RichardJ, Durr FrederickE. Development of mitoxantrone. Invest New Drugs [Internet]. 1985 [cited 2021 Jul 11];3(2). Available from: http://link.springer.com/10.1007/BF00174154

14. Hua DH, Lou K, Havens J, Perchellet EM, Wang Y, Perchellet J-P, et al. Synthesis and in vitro antitumor activity of substituted anthracene-1,4-diones. Tetrahedron. 2004 Nov;60(45):10155–63.

15. Cairns D, Michalitsi E, Jenkins TC, Mackay SP. Molecular Modelling and Cytotoxicity of Substituted Anthraquinones as Inhibitors of Human Telomerase. Bioorg Med Chem. 2002 Mar;10(3):803–7.

16. Kanokmedhakul K, Kanokmedhakul S, Phatchana R. Biological activity of Anthraquinones and Triterpenoids from Prismatomeris fragrans. J Ethnopharmacol. 2005 Sep;100(3):284–8.

17. Singh DN, Verma N, Raghuwanshi S, Shukla PK, Kulshreshtha DK. Antifungal anthraquinones from Saprosma fragrans. Bioorg Med Chem Lett. 2006 Sep;16(17):4512–4.

18. Faltynek CR, Schroeder J, Mauvais P, Miller D, Wang S, Murphy D, et al. Damnacanthal Is a Highly Potent, Selective Inhibitor of p56lck Tyrosine Kinase Activity. Biochemistry. 1995 Sep 26;34(38):12404–10.

19. Inngjerdingen M, Torgersen KM, Maghazachi AA. Lck is required for stromal cell–derived factor 1␣ (CXCL12)–induced lymphoid cell chemotaxis. 2002;99(12):8.

20. García-Vilas JA, Quesada AR, Medina MA. Damnacanthal, a noni anthraquinone, inhibits c-Met and is a potent antitumor compound against Hep G2 human hepatocellular carcinoma cells. Sci Rep. 2015 Jul;5(1):8021.

21. Weiss RB. The anthracyclines: will we ever find a better doxorubicin? Semin Oncol. 1992 Dec;19(6):670–86.

22. Randall K.Johnson. Experimental Antitumor Activity of Aminoanthraquinones.

23. Cheng CC, Zee-Cheng RKY, Narayanan VL, Ing RB, Pauli KD. The collaborative development of a new family of antineoplastic drugs. Trends Pharmacol Sci. 1981;2:223–4.

24. Cotter FE. Therapeutic milestones. Novantrone (mitozantrone). Br J Clin Pract. 1988 May;42(5):207–9.

25. Amadori S, Meloni G, Petti MC, Papa G, Miniero R, Mandelli F. Phase II trial of intermediate dose ARA-C (IDAC) with sequential mitoxantrone (MITOX) in acute myelogenous leukemia. Leukemia. 1989 Feb;3(2):112–4.

26. Satyamoorthy K, Chitnis MP, Pradhan SG, Advani SH. Modulation of Mitoxantrone Cytotoxicity by Verapamil in Human Chronic Myeloid Leukemia Cells. Oncology. 1989;46(2):128–31.

27. Durr FE, Wallace RE, Citarella RV. Molecular and biochemical pharmacology of mitoxantrone. Cancer Treat Rev. 1983 Dec;10:3–11.

28. Hoff DDV, Coltman CA, Forseth B. Activity of Mitoxantrone in a Human Tumor Cloning System. 1981;4.

29. Xie G, Zhu X, Li Q, Gu M, He Z, Wu J, et al. SZ-685C, a marine anthraquinone, is a potent inducer of apoptosis with anticancer activity by suppression of the Akt/FOXO pathway: SZ-685C induces apoptosis and inhibits tumour growth. Br J Pharmacol. 2010 Feb;159(3):689–97.

30. Zhu X, He Z, Wu J, Yuan J, Wen W, Hu Y, et al. A Marine Anthraquinone SZ-685C Overrides Adriamycin-Resistance in Breast Cancer Cells through Suppressing Akt Signaling. Mar Drugs. 2012 Mar 23;10(12):694–711.

31. Huang H-S, Chiou J-F, Fong Y, Hou C-C, Lu Y-C, Wang J-Y, et al. Activation of Human Telomerase Reverse Transcriptase Expression by Some New Symmetrical Bis-Substituted Derivatives of the Anthraquinone. J Med Chem. 2003 Jul 1;46(15):3300–7.

32. Gewirtz D. A critical evaluation of the mechanisms of action proposed for the antitumor effects of the anthracycline antibiotics adriamycin and daunorubicin. Biochem Pharmacol. 1999 Apr;57(7):727–41.

33. Minotti G, Menna P, Salvatorelli E, Cairo G, Gianni L. Anthracyclines: Molecular Advances and Pharmacologic Developments in Antitumor Activity and Cardiotoxicity. Pharmacol Rev. 2004 Jun;56(2):185–229.

34. Laurent G, Jaffrézou J-P. Signaling pathways activated by daunorubicin. Blood. 2001 Aug 15;98(4):913–24.

35. Wang J, Duncan D, Shi Z, Zhang B. WEB-based GEne SeT AnaLysis Toolkit (WebGestalt): update 2013. Nucleic Acids Res. 2013 Jul 1;41(W1):W77–83.

36. Scarpini E, Cogiamanian F. Alzheimer's disease: from molecular pathogenesis to innovative therapies. Expert Rev Neurother. 2003 Sep;3(5):619–30.

37. Stellenboom N. Comparison of the inhibitory potential towards carbonic anhydrase, acetylcholinesterase and butyrylcholinesterase of chalcone and chalcone epoxide: STELLENBOOM. J Biochem Mol Toxicol. 2019 Feb;33(2):e22240.

38. Ali TB, Schleret TR, Reilly BM, Chen WY, Abagyan R. Adverse Effects of Cholinesterase Inhibitors in Dementia, According to the Pharmacovigilance Databases of the United-States and Canada. Cavalli A, editor. PLOS ONE. 2015 Dec 7;10(12):e0144337.

39. Lolak N, Akocak S, Türkeş C, Taslimi P, Işık M, Beydemir Ş, et al. Synthesis, characterization, inhibition effects, and molecular docking studies as acetylcholinesterase, α-glycosidase, and carbonic anhydrase inhibitors of novel benzenesulfonamides incorporating 1,3,5-triazine structural motifs. Bioorganic Chem. 2020 Jul;100:103897.

40. Augustin N, Nuthakki VK, Abdullaha Mohd, Hassan QP, Gandhi SG, Bharate SB. Discovery of Helminthosporin, an Anthraquinone Isolated from Rumex abyssinicus Jacq as a Dual Cholinesterase Inhibitor. ACS Omega. 2020 Jan 28;5(3):1616–24.

41. Zengin G, Degirmenci N, Alpsoy L, Aktumsek A. Evaluation of antioxidant, enzyme inhibition, and cytotoxic activity of three anthraquinones (alizarin, purpurin, and quinizarin). Hum Exp Toxicol. 2016 May;35(5):544–53.

42. Hong C, Luo W, Yao D, Su Y-B, Zhang X, Tian R-G, et al. Novel aromatic–polyamine conjugates as cholinesterase inhibitors with notable selectivity toward butyrylcholinesterase. Bioorg Med Chem. 2014 Jun;22(12):3213–9.

43. Lee Y, Bang H, Oh J, Whang W. Bioassay-Guided Isolated Compounds from Morinda officinalis Inhibit Alzheimer's Disease Pathologies. Molecules. 2017 Sep 29;22(10):1638.

44. Tonelli M, Catto M, Tasso B, Novelli F, Canu C, Iusco G, et al. Multitarget Therapeutic Leads for Alzheimer's Disease: Quinolizidinyl Derivatives of Bi- and Tricyclic Systems as Dual Inhibitors of Cholinesterases and β-Amyloid (Aβ) Aggregation. ChemMedChem. 2015 Jun;10(6):1040–53.

45. Celik S, Ozkok F, Ozel AE, Müge Sahin Y, Akyuz S, Sigirci BD, et al. Synthesis, FT-IR and NMR characterization, antimicrobial activity, cytotoxicity and DNA docking analysis of a new anthraquinone derivate compound. J Biomol Struct Dyn. 2020 Feb 11;38(3):756–70.

46. Ozkok F, Sahin YM, Enisoglu Atalay V, Asgarova K, Onul N, Catal T. Sensitive detection of iron (II) sulfate with a novel reagent using spectrophotometry. Spectrochim Acta A Mol Biomol Spectrosc. 2020 Oct;240:118631.

47. Bingul M, Şenkuytu E, Saglam MF, Boga M, Kandemir H, Sengul IF. Synthesis, photophysical and antioxidant properties of carbazole-based bis-thiosemicarbazones. Res Chem Intermed. 2019 Sep;45(9):4487–99.

48. Stewart JJP. Application of the PM6 method to modeling the solid state. J Mol Model. 2008 Jun;14(6):499–535.

49. Stewart JJP. Application of the PM6 method to modeling proteins. J Mol Model. 2009 Jul;15(7):765–805.

50. Lee C, Yang W, Parr RG. Development of the Colle-Salvetti correlation-energy formula into a functional of the electron density. Phys Rev B. 1988 Jan 15;37(2):785–9.

51. Scalmani G, Frisch MJ. Continuous surface charge polarizable continuum models of solvation. I. General formalism. J Chem Phys. 2010 Mar 21;132(11):114110.

52. Parr RG, Pearson RG. Absolute hardness: companion parameter to absolute electronegativity. J Am Chem Soc. 1983 Dec;105(26):7512–6.

53. Pearson J, Havill DC. The Effect of Hypoxia and Sulphide on Culture-Grown Wetland and Non-Wetland Plants: II. METABOLIC AND PHYSIOLOGICAL CHANGES. J Exp Bot. 1988;39(4):431–9.

54. Gaussview 5.0.9 [Internet]. Available from: https://www.strath.ac.uk/is/software/gaussview509/

55. Gaussian 09 [Internet]. Available from: https://gaussian.com/glossary/g09/

56. Fierro C, Anderson AB, Scherson DA. Electron donor-acceptor properties of porphyrins, phthalocyanines, and related ring chelates: a molecular orbital approach. J Phys Chem. 1988 Dec;92(24):6902–7.

57. Islam N, Ghosh DC. On the Electrophilic Character of Molecules Through Its Relation with

Electronegativity and Chemical Hardness. Int J Mol Sci. 2012 Feb 17;13(2):2160–75.

58. Sen P, Yıldız SZ, Atalay VE, Kanmazalp SD, Dege N. Synthesis, molecular structure, spectroscopic and computational studies on 4-(2-(2-(2-formylphenoxy)ethoxy)ethoxy)phthalonitrile as Functionalized Phthalonitrile. Maced J Chem Chem Eng. 2019 May 24;38(1):63.

59. Enisoglu-Atalay V, Atasever-Arslan B, Yaman B, Cebecioglu R, Kul A, Ozilhan S, et al. Chemical and molecular characterization of metabolites from Flavobacterium sp. Agbor G, editor. PLOS ONE. 2018 Oct 17;13(10):e0205817.